Tibetan basement rocks near Amdo reveal "missing" Mesozoic tectonism along the Bangong suture, central Tibet

Jerome H. Guynn, Paul Kapp, Alex Pullen — Department of Geosciences, University of Arizona, Tucson, Arizona 85721, USA
Matthew Heizler — New Mexico Bureau of Geology and Mineral Resources, New Mexico Institute of Mining and Technology, Socorro, New Mexico 87801, USA
George Gehrels — Department of Geosciences, University of Arizona, Tucson, Arizona 85721, USA
Lin Ding — Institute of Tibetan Plateau Research and Institute of Geology and Geophysics, Chinese Academy of Sciences, Beijing 100029, China

ABSTRACT

The U-Pb and $^{40}Ar/^{39}Ar$ studies of a unique exposure of crystalline basement along the Jurassic–Early Cretaceous Bangong suture of central Tibet reveal previously unrecognized records of Mesozoic metamorphism, magmatism, and exhumation. The basement includes Cambrian and older orthogneisses that underwent amphibolite facies metamorphism coeval with extensive granitoid emplacement at 185–170 Ma. The basement cooled to ~300 °C by 165 Ma and was exhumed to upper crustal levels in the hanging wall of a south-directed thrust system during Early Cretaceous time. We attribute Jurassic metamorphism and magmatism to the development of a continental arc during Bangong Ocean subduction, and Early Cretaceous exhumation to northward continental underthrusting of the Lhasa terrane beneath the Qiangtang terrane. We speculate that a Jurassic arc extended regionally along the length of the Bangong suture, but in all other places in Tibet has been buried, either depositionally or structurally, beneath supracrustal assemblages.

Keywords: Tibet, Bangong suture, terrane accretion, continental arcs, continental collision.

INTRODUCTION

While it is widely assumed that the high elevation and thick crust of Tibet are largely a consequence of the Cenozoic Indo-Asian collision, the importance of older tectonism in building the Tibetan plateau and influencing its subsequent development must be considered (e.g., Yin and Harrison, 2000). Of particular relevance is the Jurassic-Cretaceous collision between the Lhasa and Qiangtang terranes along the Bangong suture in central Tibet (Fig. 1). Southward obduction of ophiolitic fragments onto the northern margin of the Lhasa terrane during Middle to Late Jurassic time is generally taken to mark the cessation of north-dipping oceanic subduction beneath the southern Qiangtang terrane and the onset of Lhasa-Qiangtang collision (Girardeau et al., 1984; Smith and Xu, 1988; Leeder et al., 1988; Zhou et al., 1997). The apparent absence of a Jurassic arc and major mid-Mesozoic tectonism along the Bangong suture has contributed to the notion that Bangong Ocean closure and subsequent Lhasa-Qiangtang collision were relatively insignificant events in the development of central Tibet (e.g., Coward et al., 1988; Dewey et al., 1988; Schneider et al., 2003). In contrast, thick accumulations of northerly derived Lower Cretaceous clastic strata in the northern Lhasa terrane (Leeder et al., 1988; Leier et al., 2004; Zhang, 2004), together with Early Cretaceous growth of an enormous, east-west–trending structural culmination in the central Qiangtang terrane (Fig. 1) (Kapp et al., 2003, 2005), have been attributed to large-magnitude northward underthrusting of the Lhasa terrane during Lhasa-Qiangtang collision. Furthermore, extensive mid-Mesozoic magmatism and exhumation have been documented along a possible extension of the Bangong suture zone in the Pamirs (Rushan-Pshart zone; Schwab et al., 2004). In an attempt to better constrain the tectonic evolution of central Tibet, we conducted geologic mapping and U-Pb and $^{40}Ar/^{39}Ar$ thermochronologic studies on unique exposures of orthogneisses and crosscutting granitoids located along the Bangong suture near Amdo (Fig. 1).

The Amdo basement is the only established exposure of pre-Mesozoic crystalline basement rock within the interior of Tibet. Earlier studies showed that the ~100-km-long by ~50-km-wide basement exposure consists of amphibolite facies orthogneisses and subordinate metasedimentary rocks intruded by undeformed granitoids (Xu et al., 1985; Harris et al., 1988b; Kidd et al., 1988; Coward et al., 1988). Conventional isotope dilution thermal ionization mass spectrometry (ID-TIMS) U-Pb dating of zircon and titanite fractions from one orthogneiss sample yielded discordant ages for both minerals, which were combined into a single discordia (Xu et al., 1985). The upper intercept age (531 ± 14 Ma) was taken to represent the crystallization age of the granitoid protolith, while the lower intercept age (171 ± 6 Ma) was interpreted to mark the timing of low-grade metamorphism due to Lhasa-Qiangtang collision; high-grade metamorphism was assumed to be related to the Cambrian magmatic emplacement (Xu et al., 1985; Coward et al., 1988). Younger intrusive granitoids (Harris et al., 1988a) were interpreted to be Early Cretaceous, on the basis of discordant U-Pb zircon ages (140–120 Ma) from one sample (Xu et al., 1985).

GEOLOGY

The Amdo basement is predominately composed of strongly foliated orthogneisses that contain small but abundant mafic amphibolite gneiss pods with the assemblage: amphibole + plagioclase + quartz + ilmenite ± biotite ± garnet. There are also sporadic outcrops of sillimanite ± garnet ± K-feldspar paragneisses and migmatites. The presence of sillimanite and K-feldspar, as well as the migmatites, suggest upper amphibolite facies metamorphic conditions. Metasedimentary rocks are exposed to the south of the orthogneiss (Fig. 2) and include marble, quartz-mica schist, phyllite, quartzite, and garnet-kyanite schist. The basement was intruded by widespread, generally undeformed granitoids (Fig. 2) of variable composition (granite, monzonite, granodiorite, quartz-syenite, and diorite).

The western boundary of the Amdo basement is a west-dipping normal fault and the northwestern boundary is a left-lateral strike-slip fault (Fig. 2), both of which cut Quaternary deposits (Coward et al., 1988; Kidd et al., 1988). The Mesozoic tectonic contacts of the northern and western exposures of the Amdo basement are buried beneath Neogene–Quaternary basin fill. Some of the granitoids, particularly in the south, have north-dipping shear zones meters to tens of meters wide that display mylonitic fabrics and bookshelf microfaulting of feldspar phenocrysts showing a top-to-the-south sense of shear. The gneisses and metasedimentary rocks along the southern margin are in the hang-

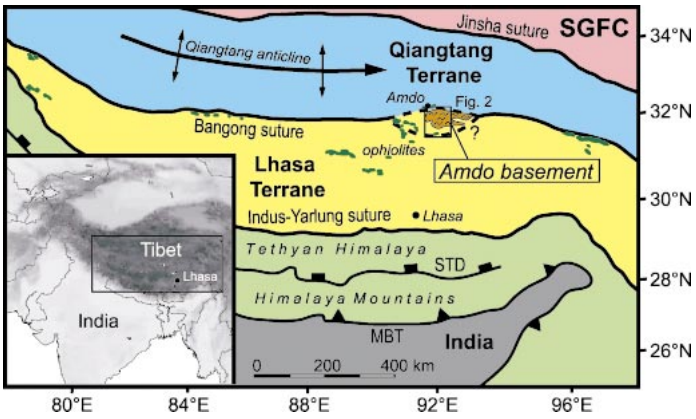

Figure 1. Map of Tibetan terranes and suture zones. Ophiolite exposures related to Bangong suture zone are shown in dark green. Note that ophiolites occur both north and south of Amdo basement. Traditionally, the Bangong suture is placed at the northernmost ophiolite outcrops, but our model suggests it occurs to the south. Abbreviations: SGFC—Songpan-Ganzi flysch complex; MBT—Main Boundary thrust; STD—South Tibetan detachment.

ing walls of north-dipping thrust fault zones with Jurassic marine shales and turbiditic sandstones and Cretaceous (?) red beds and conglomerates in the footwall.

GEOCHRONOLOGY

We dated eight granitoid samples and one orthogneiss sample using U-Pb laser-ablation multicollector inductively coupled plasma-mass

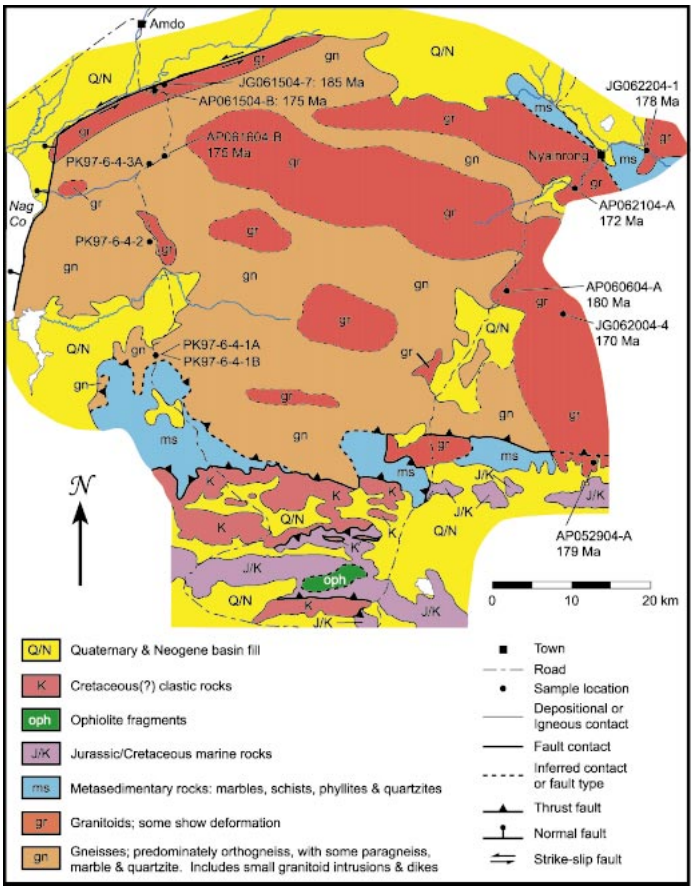

Figure 2. Simplified geologic map of western Amdo basement region. Compiled from our mapping at 1:100,000 scale and more regional geologic maps of Kidd et al. (1988) and Pan et al. (2004). For location, see Figure 1.

TABLE 1. AMDO GRANITOIDS DATED BY U-Pb LA-MC-ICPMS

Number	Lat.	Lon.	Description	Age (Ma)
JG062004-4	31.93	92.24	Porphyritic Quartz Syenite	170.7 ± 3.2
AP062104-A	32.07	92.27	Alkali-Feldspar Granite	171.8 ± 4.1
AP061504-B	32.19	91.70	Porphyritic Bi Granite	175.0 ± 3.8
AP061604-B	32.11	91.71	Bi Granite	174.0 ± 3.7
JG062204-1	32.12	92.36	Bi + Hbl Granodiorite	177.7 ± 2.5
AP052904-A	31.77	92.29	Porphyritic Quartz Syenite	177.8 ± 4.5
AP060604-A	31.96	92.16	Porphyritic Quartz Syenite	179.4 ± 3.4
JG061504-7	32.20	91.71	Bi + Hbl Granodiorite	182.9 ± 2.6

spectrometry (LA-MC-ICPMS) analyses on zircon (GSA Data Repository[1]). The crystallization ages reported in this study are based on weighted averages of concordant, clustered $^{206}Pb^*/^{238}U$ ages of individual zircons because low ^{207}Pb concentrations in young (younger than 1000 Ma) granitoids result in large uncertainties in the $^{207}Pb^*/^{235}U$ and $^{207}Pb^*/^{206}Pb^*$ ages. The assigned uncertainties (2σ) on the ages include all known random and systematic errors. The eight granitoid samples define a relatively narrow range of Middle Jurassic ages from ca. 185 Ma to ca. 170 Ma (Table 1; Table DR1; Figs. DR1A–DR1H).

The zircons from the orthogneiss sample (PK97-6-4-3A) show signs of young zircon growth due to metamorphic processes. Zircon resorption can be seen in cathodoluminescence images as bright, irregular zones only a few microns in thickness on the edges of the crystals (Fig. 3A). The wide range of discordant zircon ages (Fig. 3B; Table DR1 [see footnote 1]) is interpreted to be due to the laser beam ablating a mix of Precambrian cores and the younger rims. The younger ages correlate well with lower Th/U ratios (Fig. 3C), a typical indication of zircon (re)crystallization in equilibrium with a metamorphic fluid (Mojzsis and Harrison, 2002). The lower intercept of a discordia through the points indicates a Mesozoic age for zircon resorption. The interpreted crystallization age of 852 ± 18 Ma (Fig. 3B) provides the first direct documentation of Precambrian basement in central Tibet.

[1]GSA Data Repository item 2006094, supplementary geochronologic and thermochronologic data, is available online at www.geosociety.org/pubs/ft2006.htm, or on request from editing@geosociety.org or Documents Secretary, GSA, P.O. Box 9140, Boulder, CO 80301, USA.

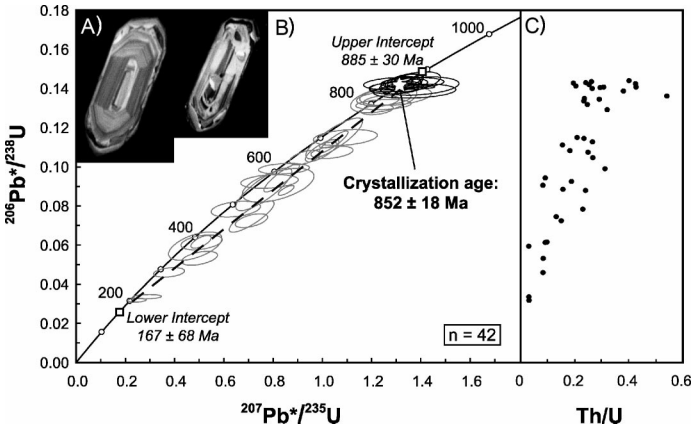

Figure 3. U-Pb analysis of orthogneiss PK97-6-4-3A. A: Cathodoluminescence images of two zircons with thin, bright resorption rims. B: U-Pb concordia diagram for orthogneiss sample PK97-6-4-3A; error ellipses are at 95% confidence level. Plotting and discordia regression are from Isoplot 3.00 (Ludwig, 2003). Analyses include laser ablation spots in cores and at tips of individual crystals. Crystallization age is based on weighted mean of $^{206}Pb^*/^{238}U$ ages for 13 concordant analyses clustered near upper intercept of discordia (older than 830 Ma; Fig. DR1i [see footnote 1]); these ellipses are shown in black. C: Variation in Th/U with $^{206}Pb^*/^{238}U$ ratio (i.e., age), showing systematic decrease in Th/U values with decreasing age.

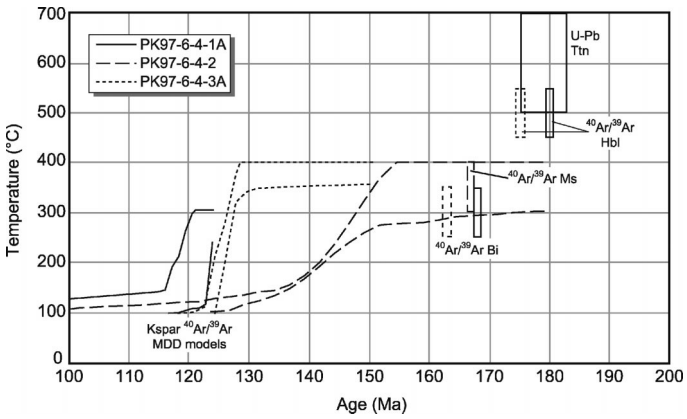

Figure 4. Cooling history of Amdo basement based on thermochronologic data from three basement samples. Ttn—titanite; Hbl—hornblende; Ms—muscovite; Bi—biotite; Kspar—K-feldspar. Lower limit of temperature range for titanite includes possibility of crystallization below closure temperature. Total gas ages of hornblende and mica are shown with assigned uncertainties of 2%. Thermal histories calculated from multidomain diffusion (MDD) modeling of K-feldspar $^{40}Ar/^{39}Ar$ age spectra represent 90% confidence window about mean of at least 20 solutions.

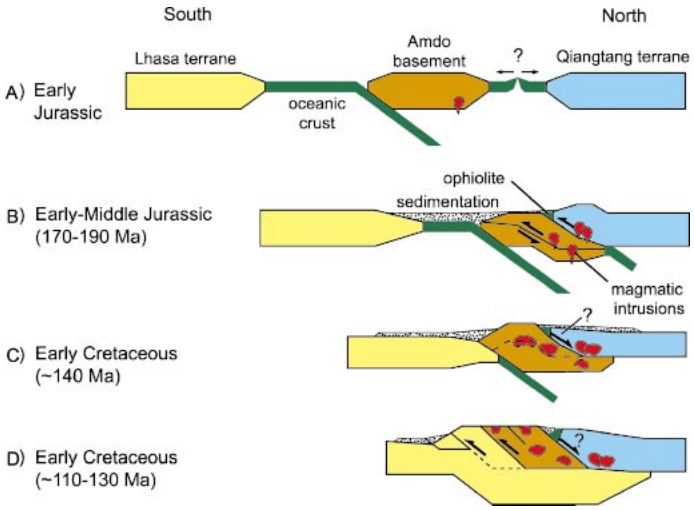

Figure 5. Tectonic model for evolution of Amdo basement and Bangong suture zone. A: Amdo basement rifted from Qiangtang terrane by Early Jurassic time, possibly due to slab rollback, creating oceanic backarc basin. B: Middle Jurassic closure of backarc basin resulted in high-grade metamorphism of Amdo basement and ophiolite obduction along northern edge of Bangong suture zone. Arc magmatism is coeval with metamorphism at this time. C: During Early Cretaceous time, Bangong Ocean closes and Lhasa terrane collides with Qiangtang terrane. Normal fault is inferred on north side of Amdo gneiss to place unmetamorphosed sedimentary rocks against high-grade Amdo basement. Foreland basin develops south of Amdo basement. D: Continued convergence between Lhasa and Qiangtang terranes in Cretaceous results in underthrusting of Lhasa terrane, exhumation of Amdo basement to upper-crustal levels, and fold-thrust belt along convergence zone.

HISTORY OF METAMORPHISM AND COOLING

We interpret the discordant analyses and metamorphic zircon rims in sample PK97-6-4-3A to indicate that the amphibolite facies metamorphism of the Amdo basement is Mesozoic. This interpretation is consistent with results of $^{40}Ar/^{39}Ar$ analysis of hornblende and U-Pb analysis of titanite from orthogneiss samples. Hornblende sample PK97-6-4-1A provides generally monotonically increasing apparent ages from ca. 160 Ma to ca. 187 Ma with an integrated age of ca. 180 Ma, while hornblende sample PK97-6-4-3A yields an integrated age of ca. 175 Ma (Fig. DR2; Table DR2 [see footnote 1]). We interpret these results to indicate that the Amdo gneisses cooled to below the bulk closure temperature for hornblende (500 ± 50 °C; McDougall and Harrison, 1999) at 180 ± 5 Ma. The U-Pb analysis on titanite from one of these samples (PK97-6-4-1A) provides a mean $^{206}Pb^*/^{238}U$ age of 179.0 ± 4.2 Ma (Fig. DR1j; Table DR1), which is statistically indistinguishable from the integrated $^{40}Ar/^{39}Ar$ hornblende age from the same sample. Given the higher closure temperature for titanite (~600–700 °C; see Frost et al., 2000, and references therein), this may indicate rapid cooling of Amdo basement ca. 180 Ma. Alternatively, the titanite may have crystallized at conditions below the closure temperature, possibly as low as 500 °C (Frost et al., 2000).

The lower temperature cooling history of Amdo basement rocks is inferred from $^{40}Ar/^{39}Ar$ thermochronologic studies on mica and K-feldspar from the orthogneiss samples (see Fig. 2 for location); the combined results are shown in Figure 4. Two biotite samples (PK97-6-4-1A and PK97-6-4-3A) and one muscovite sample (PK97-6-4-2) yield complexly varying apparent ages over the last ~80% cumulative ^{39}Ar released, but all are within the 165 ± 5 Ma age range (Fig. DR3; Table DR3), indicating regional cooling to below ~300 °C at that time.

The K-feldspar samples have complex spectra with age gradients that appear to be due largely to excess argon contamination (Fig. DR4). Isochron analysis was used to estimate initial $^{40}Ar/^{36}Ar$ trapped compositions (Fig. DR5), which were subsequently used to calculate what we refer to as isochron corrected age spectra. These isochron corrected age spectra were used to extract thermal histories using the multidiffusion domain model (Figs. DR6–DR8). Samples PK97-6-4-1A and PK97-6-4-3A show cooling from ~300 °C to ~100 °C between 135 and 115 Ma, while PK97-6-4-2 shows an older and slower episode of cooling from 155 to 125 Ma (Fig. 4). The difference in the timing of cooling initiation could be due to internal disruption of the gneiss by Early Cretaceous faults or shear zones that were not recognized in the field. Alternatively, PK97-6-4-2 displays an intermediate hump in the age spectra (both corrected and uncorrected) that could be indicative of low-temperature recrystallization, which would negate the significance of the calculated thermal history (Lovera et al., 2002). It is important to note that the absolute temperatures of the thermal histories are strongly dependent on the choice of the activation energy used, which is estimated from the step heating experiments, and may be systematically shifted to lower or higher values. This is the most probable explanation for the difference between timing of the 300 °C isotherm as determined by K-feldspar and biotite for sample PK97-6-4-3A. However, the form of the cooling histories is not affected by the choice of activation energy.

DISCUSSION AND CONCLUSIONS

Our results show that upper amphibolite facies metamorphism of the Amdo basement was the result of a tectonothermal event during the Early–Middle Jurassic and not the Cambrian, as previously inferred. Metamorphism and subsequent cooling of the Amdo basement to ~500 °C were coeval with emplacement of extensive granitoids between 185 and 170 Ma. These granitoids are the only known igneous rocks along the Bangong suture in Tibet with ages that overlap with the timing of Bangong Ocean subduction. Jurassic magmatism and exhumation have also been documented in the Pamirs along and to the north of the Rushan-Pshart suture zone, a likely westward extension of the Bangong suture zone that has been offset by the right-lateral Karakoram fault (Schwab et al., 2004). As has been suggested for the Pamir (Schwab et al., 2004), we attribute Early–Middle Jurassic metamorphism and magmatism to the development of a continental arc along the southern Qiangtang terrane due to north-dipping subduction of oceanic lithosphere. The opening and subsequent closing of a backarc oceanic basin during arc development (Figs. 5A, 5B) could explain

the presence of ophiolitic fragments north of the Amdo gneiss (Fig. 1) as well as extensive Early–Middle Jurassic marine sedimentation in the southern Qiangtang terrane and Bangong suture zone, which is apparently lacking in the Lhasa terrane (Leeder et al., 1988; Yin et al., 1988; Schneider et al., 2003). The Amdo basement and superimposed arc remained in the mid-crust until relatively rapid exhumation to upper crustal levels during the Early Cretaceous, probably due to a south-directed thrust system (Figs. 5C, 5D). This exhumation was coeval with growth of the large antiformal structural culmination in the central Qiangtang terrane (Kapp et al., 2005) and the accumulation of thick, northerly derived, clastic deposits in the Lhasa terrane (Leeder et al., 1988; Leier et al., 2004; Zhang, 2004), and is therefore attributed to Lhasa-Qiangtang continental collision. Continued northward underthrusting of the Lhasa terrane led to a southward propagation of upper crustal deformation into the northern Lhasa terrane during the Late Cretaceous, the magnitude of regional shortening exceeding 40% (Murphy et al., 1997; Kapp et al., 2003) and significant crustal thickening occurring in central Tibet (Fig. 5D). As our K-feldspar thermochronologic results indicate minimal denudation along the Bangong suture since the Early Cretaceous, this thick crust would have persisted until the onset of India's Cenozoic collision with Asia.

While the Jurassic tectonic evolution of the Bangong suture zone remains speculative, a robust conclusion is that the Amdo region provides unambiguous evidence for Jurassic high-grade metamorphism and extensive magmatism. We suggest that the Jurassic granitoids represent exhumed portions of a continental arc that paralleled the length of the Bangong suture from the Amdo area to the Pamir. This arc is ''missing'' in central Tibet because it was either buried depositionally beneath Upper Jurassic and younger supracrustal assemblages or underthrust northward beneath the Qiangtang terrane along with Lhasa terrane basement. This interpretation begs the more general question—to what extent are entire metamorphic and/or magmatic belts and other important records of tectonism ''missing'' beneath supracrustal assemblages in Tibet and in other contractional orogens worldwide?

ACKNOWLEDGMENTS

Preliminary sampling of the Amdo region was undertaken in 1997 with the assistance of A. Yin and M. Murphy. We thank R. Waldrip for assistance in the field and J. Fox and F. Guerrero for sample preparation. We benefited from discussions with M. Ducea and P.G. DeCelles and reviews by C. Burchfiel, L. Ratschbacher, and A. Yin. This research was supported by National Science Foundation grant EAR-0309844, University of Arizona start-up funds, and student research grants from ChevronTexaco and the Geological Society of America.

REFERENCES CITED

Coward, M.P., Kidd, W.S.F., Yun, P., Shackleton, R.M., and Hu, Z., 1988, The structure of the 1985 Tibet Geotraverse, Lhasa to Golmud: Royal Society of London Philosophical Transactions, ser. A, v. 327, p. 307–336.

Dewey, J.F., Shackleton, R.M., Chang, C.F., and Sun, Y.Y., 1988, The tectonic evolution of the Tibetan Plateau: Royal Society of London Philosophical Transactions, ser. A, v. 327, p. 379–413.

Frost, B.R., Chamberlain, K.R., and Schumacher, J.C., 2000, Sphene (titanite): Phase relations and role as a geochronometer: Chemical Geology, v. 172, p. 131–148, doi: 10.1016/S0009-2541(00)00240-0.

Girardeau, J., Marcoux, J., Allègre, C.J., Bassoullet, J.P., Tang, Y., Xiao, X., Zao, Y., and Wang, X., 1984, Tectonic environment and geodynamic significance of the Neo-Cimmerian Donqiao ophiolite, Bangong-Nujiang suture zone, Tibet: Nature, v. 307, p. 27–31, doi: 10.1038/307027a0.

Harris, N.B.W., Xu, R.H., Lewis, C.L., and Jin, C.W., 1988a, Plutonic rocks of the 1985 Tibet Geotraverse, Lhasa to Golmud: Royal Society of London Philosophical Transactions, ser. A, v. 327, p. 145–168.

Harris, N.B.W., Holland, T.J.B., and Tindle, A.G., 1988b, Metamorphic rocks of the 1985 Tibet Geotraverse, Lhasa to Golmud: Royal Society of London Philosophical Transactions, ser. A, v. 327, p. 203–213.

Kapp, P., Murphy, M.A., Yin, A., Harrison, T.M., Ding, L., and Guo, J.H., 2003, Mesozoic and Cenozoic tectonic evolution of the Shiquanhe area of western Tibet: Tectonics, v. 22, p. 1029, doi: 10.1029/2001TC001332.

Kapp, P., Yin, A., Harrison, T.M., and Ding, L., 2005, Cretaceous–Tertiary shortening, basin development, and volcanism in central Tibet: Geological Society of America Bulletin, v. 117, p. 865–878, doi: 10.1130/B25595.1.

Kidd, W.S.F., Pan, Y.S., Chang, C.F., Coward, M.P., Dewey, J.F., Gansser, A., Molnar, P., Shackleton, R.M., and Sun, Y.Y., 1988, Geological mapping of the 1985 Chinese-British Tibetan (Xizang-Qinghai) Plateau Geotraverse Route: Royal Society of London Philosophical Transactions, ser. A, v. 327, p. 287–305.

Leeder, M.R., Smith, A.B., and Yin, J.X., 1988, Sedimentology, palaeoecology and palaeoenvironmental evolution of the 1985 Lhasa to Golmud Geotraverse: Royal Society of London Philosophical Transactions, ser. A, v. 327, p. 107–143.

Leier, A.L., Eisenberg, D.A., Kapp, P., and DeCelles, P.G., 2004, Evidence of Cretaceous foreland basin systems in the Lhasa terrane and implications for the tectonic evolution of southern Tibet: Eos (Transactions, American Geophysical Union), v. 85, abs. T53A–467.

Lovera, O.M., Grove, M., and Harrison, T.M., 2002, Systematic analysis of K-feldspar $^{40}Ar/^{39}Ar$ step heating results II: Relevance of laboratory argon diffusion properties to nature: Geochimica et Cosmochimica Acta, v. 66, p. 1237–1255, doi: 10.1016/S0016-7037(01)00846-8.

Ludwig, K.R., 2003, Isoplot 3.00: Berkeley Geochronology Center Special Publication 4, 70 p.

McDougall, I., and Harrison, T.M., 1999, Geochronology and thermochronology by the $^{40}Ar/^{39}Ar$ method (second edition): Oxford, Oxford University Press, 269 p.

Mojzsis, S.J., and Harrison, T.M., 2002, Establishment of a 3.83-Ga magmatic age for the Akilia tonalite (southern West Greenland): Earth and Planetary Science Letters, v. 202, p. 563–576, doi: 10.1016/S0012-821X(02)00825-7.

Murphy, M.A., Yin, A., Harrison, T.M., Dürr, S.B., Chen, Z., Ryerson, F.J., Kidd, W.S.F., Wang, X., and Zhou, X., 1997, Did the Indo-Asian collision alone create the Tibetan plateau?: Geology, v. 25, p. 719–722, doi: 10.1130/0091-7613(1997)025<0719:DTIACA>2.3.CO;2.

Pan, G., Ding, J., Yao, D., and Wang, L., 2004, Geological map of the Qinghai-Xizang (Tibet) Plateau and adjacent areas: Chengdu, China, Chengdu Cartographic Publishing House, scale 1:1,500,000.

Schneider, W., Mattern, F., Wang, P., and Li, C., 2003, Tectonic and sedimentary basin evolution of the eastern Bangong-Nujiang zone (Tibet): A Reading cycle: International Journal of Earth Sciences, v. 92, p. 228–254.

Schwab, M., Ratschbacher, L., Siebel, W., McWilliams, M., Minaev, V., Lutkov, V., Chen, F., Stanek, K., Nelson, B., Frisch, W., and Wooden, J.L., 2004, Assembly of the Pamirs: Age and origin of magmatic belts from the southern Tien Shan to the southern Pamirs and their relation to Tibet: Tectonics, v. 23, p. TC4002, doi: 10.1029/2003TC001583.

Smith, A.B., and Xu, J.T., 1988, Paleontology of the 1985 Tibet Geotraverse, Lhasa to Golmud: Royal Society of London Philosophical Transactions, ser. A, v. 327, p. 53–105.

Xu, R.H., Schärer, U., and Allègre, C.J., 1985, Magmatism and metamorphism in the Lhasa block (Tibet): A geochronological study: Journal of Geology, v. 93, p. 41–57.

Yin, A., and Harrison, T.M., 2000, Geologic evolution of the Himalayan-Tibetan orogen: Annual Review of Earth and Planetary Sciences, v. 28, p. 211–280, doi: 10.1146/annurev.earth.28.1.211.

Yin, J.X., Xu, J.T., Liu, C.J., and Li, H., 1988, The Tibetan Plateau—Regional stratigraphic context and previous work: Royal Society of London Philosophical Transactions, ser. A, v. 327, p. 5–52.

Zhang, K.-J., 2004, Secular geochemical variations of the Lower Cretaceous siliciclastic rocks from central Tibet (China) indicate a tectonic transition from continental collision to back-arc rifting: Earth and Planetary Science Letters, v. 229, p. 73–89, doi: 10.1016/j.epsl.2004.10.030.

Zhou, M.-F., Malpas, J., Robinson, P.T., and Reynolds, P.H., 1997, The dynamothermal aureole of the Donqiao ophiolite (northern Tibet): Canadian Journal of Earth Sciences, v. 34, p. 59–65.

Manuscript received 21 November 2005
Revised manuscript received 20 January 2006
Manuscript accepted 23 January 2006

Printed in USA

Geology

Tibetan basement rocks near Amdo reveal "missing" Mesozoic tectonism along the Bangong suture, central Tibet

Jerome H. Guynn, Paul Kapp , Alex Pullen, Matthew Heizler, George Gehrels and Lin Ding

Geology 2006;34;505-508
doi: 10.1130/G22453.1